AGU ADVANCING EARTH AND SPACE SCIENCES

Geophysical Research Letters

RESEARCH LETTER
10.1029/2025GL121465

Emergence of Subsurface Warming in the Southern Ocean Gateway Between New Zealand and Antarctica

A. I. Ferola[1,2], **Y. Cotroneo**[1], **P. Castagno**[3], **G. Fusco**[1], **P. Falco**[4], **G. Budillon**[1], **E. Zambianchi**[5], and **G. Aulicino**[1]

[1]Department of Science and Technology, University of Napoli Parthenope, Napoli, Italy, [2]European Space Agency, ESRIN, Frascati, Italy, [3]Department of Mathematical and Computer Sciences, Physical Sciences and Earth Sciences, University of Messina, Messina, Italy, [4]Department of Life and Environmental Sciences, Marche Polytechnic University, Ancona, Italy, [5]Department of Earth Sciences, Università di Roma "la Sapienza", Roma, Italy

Key Points:

- Subantarctic Mode Water and Antarctic Intermediate Water exhibit significant subsurface warming from 1994 to 2025
- Recent years show an acceleration of warming in both water masses, exceeding long-term trends
- These changes underscore the need for sustained high-resolution observations in key Southern Ocean gateways

Supporting Information:

Supporting Information may be found in the online version of this article.

Correspondence to:

G. Aulicino and Y. Cotroneo,
giuseppe.aulicino@uniparthenope.it;
yuri.cotroneo@uniparthenope.it

Citation:

Ferola, A. I., Cotroneo, Y., Castagno, P., Fusco, G., Falco, P., Budillon, G., et al. (2026). Emergence of subsurface warming in the Southern Ocean gateway between New Zealand and Antarctica. *Geophysical Research Letters*, *53*, e2025GL121465. https://doi.org/10.1029/2025GL121465

Received 21 DEC 2025
Accepted 2 JUN 2026

Author Contributions:

Conceptualization: A. I. Ferola, G. Aulicino
Data curation: A. I. Ferola, Y. Cotroneo, G. Aulicino
Formal analysis: A. I. Ferola, G. Aulicino
Funding acquisition: G. Budillon
Investigation: P. Castagno, P. Falco, G. Aulicino
Methodology: A. I. Ferola, Y. Cotroneo, G. Aulicino
Supervision: G. Aulicino
Writing – original draft: A. I. Ferola, G. Aulicino
Writing – review & editing: Y. Cotroneo, P. Castagno, G. Fusco, P. Falco, G. Budillon, E. Zambianchi

Abstract We analyze temperature variability in the surface and intermediate layers of the Southern Ocean from 1994 to 2025 using a 30-year summertime record of Expendable Bathythermograph (XBT) measurements collected along the PX36 line across the New Zealand–Antarctica chokepoint of the Antarctic Circumpolar Current (ACC). Significant subsurface warming emerges along the northern flank of the current, while waters south of the Polar Front exhibit no long-term trend. Within the main water masses of the region, Subantarctic Mode Water and Antarctic Intermediate Water warm by ~0.22 and ~0.16°C decade^{-1} respectively, driven largely by strong temperature increase during the last decade. These results reveal this chokepoint as a hotspot of Antarctic Intermediate Water variability and suggest warming in its upstream source regions, underscoring the need for sustained, high-resolution monitoring of this key sector of the Southern Ocean.

Plain Language Summary The Southern Ocean plays a key role in regulating Earth's climate by absorbing heat and carbon and connecting all major ocean basins. However, this region is warming rapidly, especially in the north, where the Antarctic Circumpolar Current flows. In this study, we analyzed 30 years of temperature measurements collected each summer along a ship route between New Zealand and Antarctica. These observations show that two important water masses—Subantarctic Mode Water and Antarctic Intermediate Water—have warmed significantly over the past three decades, with the strongest changes occurring in the last 10 years. These water masses spread heat into the deeper ocean and toward lower latitudes, so their warming has global consequences. In contrast, waters closer to Antarctica show little or no long-term warming. Overall, our results point to a clear hotspot of ocean warming in the northern part of the Southern Ocean. This warming highlights the need for continuous, high-quality monitoring to better understand how the Southern Ocean is changing and what this means for the global climate system.

1. Introduction

Covering more than a quarter of the global ocean surface (Gille, 1994), the Southern Ocean (SO) represents a pivotal component of the global overturning circulation, primarily owing to the presence of dense water formation and inter-basin exchange driven by the Antarctic Circumpolar Current (ACC) (Rintoul, 2018). During the last decades, the SO has experienced a substantial warming trend, which has been further intensified by Antarctic stratospheric ozone depletion, at least until the early 21st century, and by the increasing concentration of atmospheric CO_2 (W. Liu et al., 2022). Despite projections indicating both ozone recovery and depletion (Zambri et al., 2021), fluxes of radiative heat and freshwater in the SO are expected to increase due to enhanced precipitation, ice melting and a poleward intensification of the SO westerlies. This warming trend has profound implications for the melting of the Antarctic ice shelf and ice sheet, for sea-level rise, and for remote circulations such as the intertropical convergence zone and tropical ocean-atmosphere circulations, which in turn affect extreme weather events, agriculture, and ecosystems (Cai et al., 2023). The heating of the SO also influences its capacity to store soluble gases, including CO_2 (Gille, 2002). Furthermore, several studies have demonstrated greater warming in the northern portion of the ACC compared to the water masses south of the Polar Front, which experience comparatively less warming or even cooling (Armour et al., 2016; Auger et al., 2021; Sallée, 2018). Although the main mechanisms driving the dynamics of SO and ACC have been highlighted in the last decades (Falco & Zambianchi, 2011; Menna et al., 2020; Olbers et al., 2004; Rintoul, 2018; Thompson & Naveira Garabato, 2014), many fundamental questions remain unanswered. These include the interactions between ice

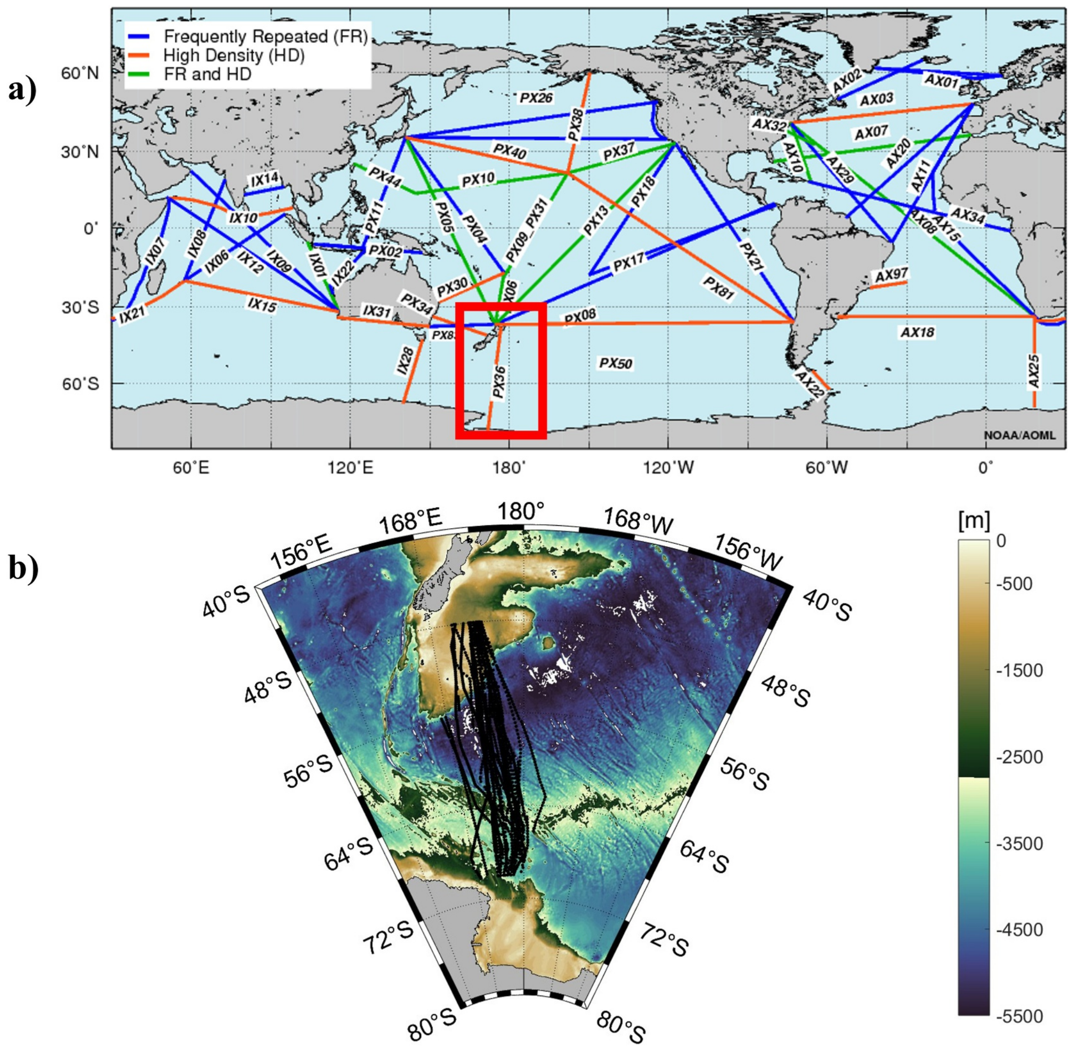

Figure 1. (a) XBT Network distribution map (https://www.aoml.noaa.gov/proj/xbt-network). Red box identifies the PX36 monitoring line area. (b) Bathymetry map of the Southern Ocean region stretching between New Zealand and Antarctica (PX36 transect). The black dots show the locations where XBT casts were carried out between December 1994 and January 2025. Only data collected between 48° and 70°S were selected.

shelves and ice sheets, the influence of oceanic eddies, the dynamics of tropical-polar interactions, and the impact of the SO response on climate change forcing itself (Abram et al., 2025; Ferola et al., 2023). The progress in understanding these processes is hindered by limited observations and the low resolution of climate models. Therefore, there is a pressing need for extensive and long-term observations to shed light on these uncertainties (Auger et al., 2021; Budillon & Rintoul, 2003). In this study, we analyze 30 years of observations gathered in the ACC, through the repeated collection of Expendable Bathythermograph (XBT) measurements along the PX36 monitoring line south of New Zealand. Figure 1a shows the global XBT monitoring line distribution highlighting the PX36, which is then reported in detail in Figure 1b. Our analysis focuses on the long-term variability of temperature changes and trends within the principal water masses of the ACC over the past three decades, presenting the first observational evidence of an accelerated subsurface warming of Subantarctic Mode Water (SAMW) and Antarctic Intermediate Water (AAIW) at the New Zealand–Antarctica gateway, and identifying this region as a key hotspot of recent SO change. This assessment provides a baseline for future investigations into temperature variability across depth, latitude, and time within the study area, as well as its implications for the broader SO.

10.1029/2025GL121465

2. Data and Methods

2.1. XBT Data

In this study, we use a 30-year record of XBT hydrographic observations collected along the PX36 transect south of New Zealand (48°–70°S) during austral summers from 1994/95 to 2024/25 (Figure S1 in Supporting Information S1). Profiles were acquired with Sippican T7 probes (vertical resolution 0.65 m; nominal depth 760 m) during cruises of the Italian R/V Italica and Laura Bassi, and the Korean R/V Araon, within the Italian National Research Program in Antarctica (PNRA) CLIMA, SOChIC, and MORSea projects. Temperature profiles were interpolated onto a 1 m vertical grid and a 1/8° latitude grid to construct mean summer sections. Quality control followed AOML/NOAA procedures (Cowley & Krummel, 2022; Tan et al., 2023), with outliers removed, and profiles flagged by reliability class; only data marked as good or probably good were used. Temperature and depth values were bias-corrected for probe type and calendar year to enable robust trend analysis. The full data set is publicly available at https://zenodo.org/records/14848849. A full description of the applied QC and correction methodologies is provided in Aulicino, Ferola, et al. (2025). These observations have also been used in the development of a high-resolution boundary current product based on gridded XBT transects (Goes et al., 2026).

On this basis, temperature trends over 1994–2025 were computed using linear regression at each grid point, with the signal-to-noise ratio (S = trend/interannual variability) calculated to assess trend significance (Figure S2 in Supporting Information S1).

$$S = \frac{ny * a}{\mathrm{STD}(ax - T)}$$

where n is the number of years, y is the time index, a is the linear regression slope, T is the temperature anomaly for a specific time index and STD is the standard deviation of residuals. Additional tests evaluating the sensitivity of the trends to ship-track variability and spatial sampling are described in Text S1 in Supporting Information S1.

2.2. SAMW Sea Surface Temperature Trend From ERA5 Reanalysis

ERA5 monthly sea-surface temperature (SST) fields (Hersbach et al., 2023) for January–February were extracted over the SAMW domain (170°E−180°, 46°–54°S), consistent with the period and region of in situ sampling. For each year, SSTs were averaged over both months and across the domain to obtain a single seasonal value. Linear trends were then computed using the same regression approach applied to the XBT temperatures.

3. Results

3.1. Mean Structure, Variability, and Frontal Positions

Based on the XBT data collected along the PX36 transect, we computed the climatological mean temperature and its standard deviation for the study period (Figures 2a and 2b). Afterward, ACC fronts (i.e., Northern Sub-Antarctic Front - NSAF, Southern Sub-Antarctic Front - SSAF, Polar Front - PF, southern ACC front - sACCf) were located using established hydrographic criteria (Budillon & Rintoul, 2003; Orsi et al., 1995; Sokolov & Rintoul, 2007) and further refined using satellite Sea Surface Height to minimize uncertainties associated with eddies and frontal meanders. Temperature standard deviations reveal enhanced variability near the NSAF and over major topographic features such as the Campbell Plateau, consistent with intensified eddy activity and frontal variability (Figure 2b).

Water masses (i.e., SAMW, AAIW, Antarctic Surface Water - AASW, and Circumpolar Deep Water—CDW; Carter et al., 2022; de Brauwere et al., 2007) were also identified using core temperature, salinity, and density values derived from Argo floats (2003–2024) and WOA climatology (2005–2017) (Figure S3 in Supporting Information S1), allowing the definition of climatological water-mass residence regions along PX36 (Figure 2). SAMW occupies the upper ~200 m north of the NSAF, shallower than in adjacent regions (e.g., Auger et al., 2021). This vertical confinement and spatial configuration are consistent with recent SO–wide evidence of progressive SAMW shoaling and warming, particularly in the Pacific sector, driven by enhanced surface buoyancy forcing and altered subduction pathways (Wyatt et al., 2025). AAIW lies below ~400 m between the northern and southern branches of the SAF. Its origin is generally associated with subduction processes occurring

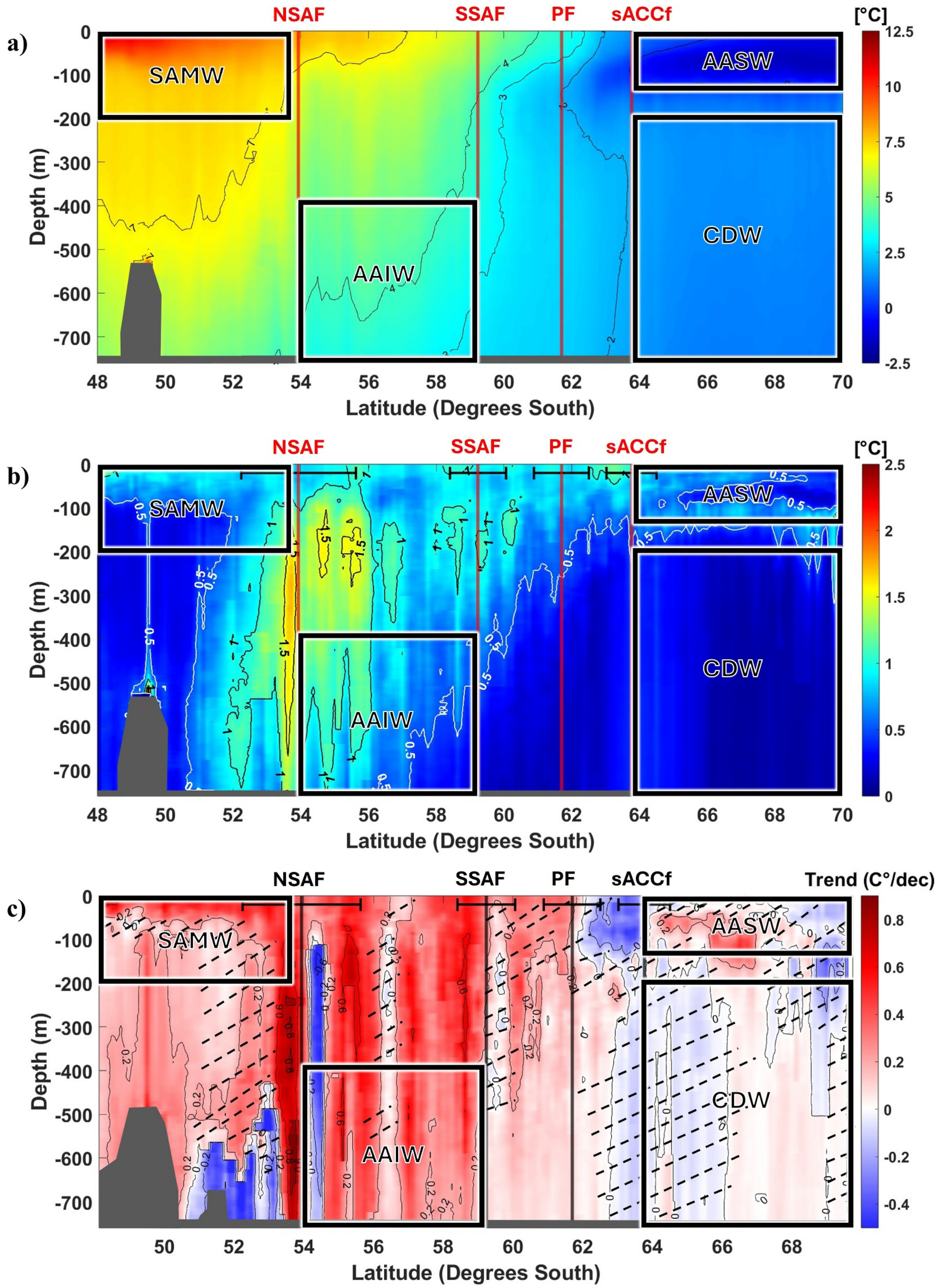

Figure 2. (a) Mean summer temperature section along the New Zealand–Antarctica PX36 transect from XBT profiles collected between December 1994 and January 2025. (b) Standard deviation of temperature. (c) Linear temperature trends (°C decade^{-1}). In all panels, black boxes mark the climatological cores of the main water masses identified from Argo floats (see Water Masses Identification and Trend in Methods). In panels (a and b), the Antarctic Circumpolar Current fronts are shown as red vertical lines, whereas in (c) they are shown as black vertical lines; horizontal bars indicate the latitudinal standard deviation of front positions. Front locations are filtered to reduce the influence of eddies and meanders. Regions without data because topography is masked in dark gray. In (c), dashed black lines sloping upward to the right highlight trends that are less significant than the interannual variability within each water mass.

north of the PF (Orsi et al., 1995). AASW is found at depths shallower than 150 m south of the PF, whereas CDW, the largest and most voluminous SO water mass, occupies depths exceeding 200 m south of the sACCf.

To assess the reliability of our data set, we analyzed the temperature standard deviation along PX36. The results are illustrated in Figure 2b, where the mean positions of the ACC fronts are superimposed on the latitudinal section. Overall, the standard deviations remain ~1°C in the upper 100 m across the transect and decrease to less than 0.5°C at greater depths, except in proximity to ACC fronts where variability is enhanced (Budillon & Rintoul, 2003; Cotroneo et al., 2013; Freeman et al., 2016; Sokolov & Rintoul, 2009a, 2009b), peaking near the NSAF. This elevated variability likely reflects a combination of factors, including the large latitudinal excursions of the NSAF as the northernmost ACC front, the influence of complex bathymetry south of New Zealand (Macquarie Ridge and Campbell Plateau) (X. Liu et al., 2024), and mesoscale eddy activity (Cotroneo et al., 2013; Ferola et al., 2023; Fu et al., 2010; Lu & Speer, 2010; Sallée et al., 2011; Thompson & Sallée, 2012). Variations in ship tracks across the Campbell Plateau may also contribute to uncertainty in the inferred NSAF position (Figure 1b). Notably, the temperature standard deviation near frontal positions has increased over the past two decades (Figure S4 in Supporting Information S1), indicating intensified mesoscale variability and a possible shift in the regional dynamical regime (Cotroneo et al., 2013).

To further investigate this variability, temperature anomalies were calculated for each cruise (Figure S5 in Supporting Information S1). Anomaly sections reveal pronounced interannual variability across latitudinal zones, with the largest anomalies concentrated near the NSAF, likely reflecting mesoscale eddy activity. These signals likely reflect eddy activity, introducing anomalies up to ±3°C. Recurring features, such as the cold tongue of AASW extending toward the sACCf, are also evident. Moving from northern to southern fronts, the intensity of temperature standard deviation signal decreases and affects progressively shallower portions of the surface layer (Figure 2b). This latitudinal gradient likely arises from larger frontal displacements at the northern ACC boundary and/or intrinsically lower thermal variability in southern waters, consistent with basin-scale findings showing that SAMW dominates upper-ocean thermal variability north of the SAF (Wyatt et al., 2025).

However, interannual variability observed near the NSAF and across the northern ACC flank is likely influenced not only by mesoscale eddy activity, but also by large-scale modes of atmospheric variability that modulate wind forcing and frontal position in the Pacific sector of the SO. Variability associated with the Southern Annular Mode (SAM) alters the strength and latitude of the Southern Hemisphere westerlies, leading to meridional shifts of ACC fronts and changes in upper-ocean circulation (Fogt & Marshall, 2020). Positive SAM phases, which have been enhanced in recent decades, are associated with intensified and poleward-shifted westerlies and increased surface heat uptake in the Subantarctic Zone (G. Wang et al., 2017). This signal may be particularly evident near the NSAF because atmospheric anomalies interact there with a dynamically complex northern ACC flank, where bathymetric steering, frontal meandering, mesoscale eddies, and exchanges with subtropical source waters can amplify temperature variability and affect SAMW/AAIW formation pathways. Additionally, the Antarctic Circumpolar Wave (ACW) may also influence atmospheric variability and water mass properties across several timescales (Cerrone, Fusco, Cotroneo, et al., 2017; Cerrone, Fusco, Simmonds, et al., 2017). These large-scale modes likely modulate the background dynamical state upon which mesoscale eddies operate, amplifying interannual temperature variability and frontal meandering near the NSAF (Sallée et al., 2021). Farther south, variability is increasingly controlled by polar processes including sea-ice dynamics, deep overturning circulation, and CDW upwelling, which tend to damp or obscure the direct influence of subtropical atmospheric teleconnections.

3.2. Long-Term Temperature Trends

Temperature trends along PX36 over the past three decades are shown in Figure 2c. A coherent warming signal emerges across much of the transect, consistent with earlier reports of upper-1,000 m warming in the SO (Gille, 2008) and more recent trends along the Hobart–Dumont D'Urville section (Auger et al., 2021), immediately west of our study area. The strongest warming occurs in the northernmost sector of the transect, reaching +0.8°C decade^{-1}, whereas the southern portion of the section shows weaker trends, ranging between −0.2 and +0.2°C decade^{-1}, and higher interannual variability. These patterns align with Armour et al. (2016), who reported pronounced upper-ocean warming along the northern flank of the ACC (40°–50°S) and slower warming (or even cooling) farther south. Regions where the trend is smaller than interannual variability ($S < 1$) are indicated with dashed black lines in Figure 2c, highlighting areas of low trend significance. Interannual variability often prevails in the southernmost sector and near the NSAF, consistent with the large standard deviations shown in Figure 2b. Nevertheless, statistically significant positive trends persist between ∼48°S and the SSAF, confirming the observed ocean warming in the northernmost sector. This latitudinal gradient mirrors basin-scale observations indicating that SAMW dominates upper-ocean thermal variability north of the NSAF, whereas AAIW exhibits more muted variability associated with its role as an integrator of upstream mode-water changes.

3.3. Water-Mass Temperature 30-Year Trends

To further investigate temperature changes, we computed mean summer temperatures and anomalies for each water mass relative to 1994–2025. Linear trends were estimated where data coverage exceeded 70% of the time series, and statistical significance was assessed using the Mann-Kendall test. The strongest and most significant trends occur in the northern ACC sector, with SAMW warming at +0.22°C decade^{-1} ($p \leq 0.01$) and AAIW at +0.16°C decade^{-1} ($p \leq 0.05$) (Figures 3a, 3c, 3e, and 3g). These values are consistent with previous estimates of AAIW warming (+0.05 to +0.15°C decade^{-1}) since the mid-1970s (Schmidtko & Johnson, 2012). The magnitude and persistence of SAMW warming are also consistent with SO assessments by Wyatt et al. (2025), who demonstrate sustained SAMW warming and density reduction over recent decades, making it a disproportionate contributor to regional heat uptake. AAIW warming similarly reflects basin-scale coherence, largely inherited from its SAMW precursor, confirming that AAIW warming primarily reflects changes in surface-forced mode waters rather than local air–sea interaction. The warming of SAMW and AAIW is broadly attributable to anthropogenic greenhouse gas (GHG) forcing (Bilbao et al., 2019; Swart et al., 2018), as surface heat flux anomalies induced by GHGs are absorbed at the ocean surface around 50°–60°S and subsequently transported into the subsurface (Cai et al., 2010; Cheng et al., 2022; Shi et al., 2018). Wyatt et al. (2025) further note that SAMW warming is accompanied by increased stratification, with implications for ventilation efficiency and downstream thermocline structure. In contrast, southern water masses (AASW and CDW) exhibit weak or negligible trends. AASW, strongly influenced by sea-ice melt and atmospheric forcing, has a relatively short residence time and high temporal variability, which makes it susceptible to rapid changes in temperature and composition, and complicates the detection of long-term trends. CDW, shaped by mixing among deep waters from the three major ocean basins, remains relatively stable along PX36, despite warming reported in adjacent regions. CDW trends along PX36 appear weaker than those reported by Auger et al. (2021), who analyzed Upper Circumpolar Deep Water (UCDW) along the Hobart–Dumont D'Urville transect (140–150°E) over 1992–2017. That section crosses a region strongly influenced by topographic interactions downstream of the Southeast Indian Ridge. Differences between the two studies may therefore reflect zonal heterogeneity in UCDW warming within the ACC, as well as differences in the definition of the CDW layer considered and the analysis period.

3.4. Water-Mass Temperature Decadal Evolution

Dividing the XBT record into three decades (1994/95–2003/04, 2004/05–2013/14, 2014/15–2024/25) reveals a clear acceleration of warming in recent years, though statistical significance varies among water masses (Figures 3b, 3d, 3f, and 3h). SAMW, the northernmost water mass, shows positive trends in all decades, increasing progressively to +0.96°C decade^{-1} ($p \leq 0.05$) in the most recent decade. This acceleration is consistent with enhanced SAM driven wind forcing and increased surface heat uptake since the early 2010s (Wyatt et al., 2025). AAIW shows limited change during the first two decades but undergoes pronounced warming (+1.31°C decade^{-1}, $p \leq 0.05$) in 2014/15–2024/25, strongly influencing its 30-year trend. These estimates exclude data from the last two oceanographic cruises (white dots in Figure 3d), due to insufficient XBT data coverage in the AAIW region. In contrast, CDW shows no clear trend, while AASW presents a less regular behavior, stable in the first decade (1994/95–2003/04), positive in 2004/05–2013/14, and negative in 2014/15–2024/25, yielding no significant long-term trend.

Surface warming within SAMW was further evaluated using ERA5 SST reanalysis coinciding with XBT sampling. Results show a significant increase of ∼1.08°C over the last decade (Figure S6 in Supporting Information S1), corroborating the XBT-derived trends and supporting an air–sea forcing origin. Subduction of SAMW contributes to AAIW warming, particularly near the Campbell Plateau, a known key formation region. Overall, the northern ACC flank emerges as a robust warming hotspot, whereas southern regions remain characterized by weaker trends and stronger interannual variability. The observed SAMW and AAIW trends likely result from a combination of anthropogenic forcing, enhanced surface heat fluxes, and evolving SO stratification, with potential implications for heat and carbon transport to lower latitudes.

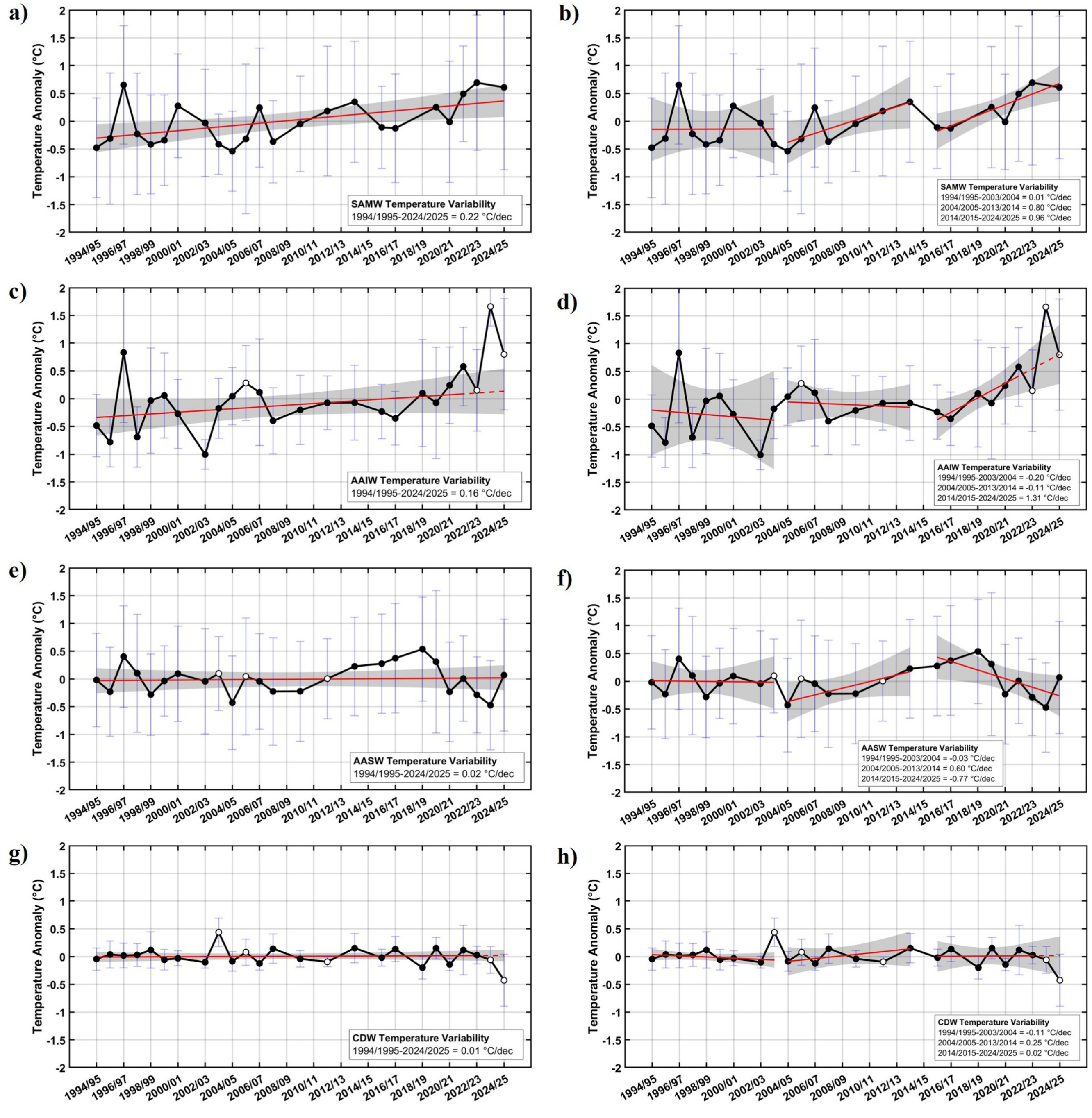

Figure 3. Mean summer temperature anomalies of SAMW (a, b), AAIW (c, d), AASW (e, f), and CDW (g, h) between the austral summers of 1994/1995 and 2024/2025. Panels (a, c, e, g) show the anomalies with a single linear trend fitted over the full study period, whereas panels (b, d, f, h) show the same anomalies with separate linear trends for each of the three decades (1994/95–2003/04, 2004/05–2013/14, 2014/15–2024/25). The solid red line(s) represent the linear temperature trend(s), expressed in °C decade^{-1}; the gray shaded area indicates the 95% confidence interval. Blue vertical lines show the standard deviation of the mean temperature values obtained for each austral summer. White dots mark water-mass temperature values that are not statistically significant and were excluded from trend calculations.

4. Conclusion and Discussion

The SO is among the oceans most strongly affected by global warming, yet this warming is spatially heterogeneous (Cheng et al., 2022; Roemmich et al., 2015; Sallée, 2018). Based on 30 years of XBT observations in the SO Pacific sector, our study unveils a pronounced warming along the northern ACC flank (Figure 2c), underscoring the critical contributions of SAMW and AAIW (+0.22 and +0.16°C decade^{-1}, respectively, with particularly strong warming over the last decade) to global ocean heat accumulation over the last three decades. While SO warming has been widely documented, our results provide the first long-term observational evidence of accelerated subsurface warming emerging at a major ACC gateway, revealing spatially localized amplification not resolved in basin-averaged products. These results are consistent with recent basin-scale assessments identifying SAMW as one of the SO water masses exhibiting the highest interannual temperature variability, reflecting its strong coupling to atmospheric forcing and frontal displacement along the northern ACC boundary (Wyatt et al., 2025). Together, our results provide new regional evidence for the contrasting thermal responses of key ACC water masses and reinforce previously reported SO warming rates. Auger et al. (2021) report comparable warming within the ACC (+0.2 to +0.8°C decade^{-1}) along the Hobart–Dumont D'Urville section, while Li et al. (2023), using global Argo data (2005–2020), identified an accelerated ocean heat uptake particularly within mode and intermediate waters, suggesting that the two northernmost water masses of the SO (i.e., SAMW and AAIW) contribute ∼36% of global ocean warming. Consistent with these findings, Wyatt et al. (2025) identify SAMW as a primary contributor to SO upper-ocean warming, exhibiting statistically robust positive trends since the 1990s, particularly in the Pacific and Indian sectors, in agreement with the regional patterns observed along PX36. Wyatt et al. (2025) further highlight the role of AAIW as a key intermediary in the SO heat uptake pathway, integrating SAMW-driven surface warming and redistributing heat into the subtropical and tropical thermocline.

In contrast, our findings show little long-term change for CDW, therefore not supporting widespread warming or shoaling of Upper Circumpolar Deep Water along PX36, as previously reported at other ACC chokepoints (e.g., Auger et al., 2021; Hu et al., 2025). However, modeling results (Naughten et al., 2023) suggest that changes in the properties of the CDW core in the open SO are relatively small (∼0.2°C warming over the 21st century), supporting the idea that the observed warming of the Antarctic continental shelf is indeed driven by an increased volume of CDW intrusions rather than by a rise in CDW temperature.

ERA5 SST reanalysis indicates that SAMW surface warming (∼1.08°C over the last decade; Figure S6 in Supporting Information S1) is largely air–sea driven, reinforcing the interpretation that SAMW acts as a major pathway linking atmospheric forcing to subsurface ocean heat uptake. Subduction of SAMW into AAIW (Li et al., 2022) explains the coupled warming of AAIW (Li et al., 2021, 2022; Z. Wang et al., 2025). Additionally, Li et al. (2021) documented strong subduction of SAMW near the Campbell Plateau (170°E), where Z. Wang et al. (2025) highlighted a key formation region for AAIW. As a result, SAMW warming is efficiently transmitted to AAIW, leading to a pronounced temperature increase in both water masses, particularly during the most recent decade in our study area. Recent findings further indicate that the evolution observed along the northern ACC flank is embedded within a broader wind-driven reorganization of the SO system, with large sectors of the polar SO shifting since ∼2015 toward saltier surface conditions, reduced stratification, and enhanced vertical exchange of subsurface heat (Silvano et al., 2025). This transition suggests that strengthened atmospheric forcing may be altering both upper-ocean ventilation and the accessibility of subsurface heat reservoirs. Such changes are expected to be particularly relevant along the ventilated Subantarctic sectors, where SAMW and AAIW formation are closely coupled to surface buoyancy fluxes, wind forcing, and mixed-layer dynamics. Farther south of the PF, however, the same basin-scale forcing is mediated by a polar dynamical regime in which upper-ocean variability is more strongly shaped by sea ice-ocean interactions and overturning processes, potentially weakening the coherence of a surface-intensified warming signal. Thus, the presented trends likely reflect the combined imprint of intensified atmospheric forcing, frontal variability, and evolving vertical structure under changing SO conditions.

Therefore, our results provide independent observational evidence consistent with an active SAMW–AAIW transformation pathway in the Campbell Plateau sector, although the identification of this region as a primary AAIW formation site requires further confirmation. This emerging hotspot of anomalously warm AAIW has potential global implications. As AAIW ventilates large portions of the subtropical and tropical thermocline, the injection of warmer waters from the SO could enhance heat storage in the ocean interior, altering stratification, and potentially reducing the efficiency of carbon uptake (Li et al., 2023; Meijers et al., 2023). Moreover, the export of warmer AAIW from the New Zealand–Antarctica chokepoint may impact basin-scale circulation, climate variability in the Pacific and beyond (Cai et al., 2023), with possible downstream effects on the meridional overturning circulation and global sea-level rise.

Mesoscale eddies dominate short-timescale variability along the northern ACC flank, while climate-mode-driven wind forcing modulates frontal displacement on interannual scales. The enhanced variability and recent warming observed in this sector therefore reflect the combined effects of intensified mesoscale activity and large-scale atmospheric forcing, including variability in the SAM and Pacific climate teleconnections, which influence frontal positions and surface heat uptake in the Subantarctic Zone (Gille, 2014; Purich & England, 2021). Climate-mode variability modulates surface forcing and largely explains short-term fluctuations and frontal displacements. However, the persistent multi-decadal warming and recent acceleration observed in SAMW and AAIW are more consistent with longer-term changes in the mean state of surface forcing and ventilation pathways in the upstream SO (Li et al., 2021).

Collectively, these findings indicate an ongoing SO state transition that may already be reshaping global heat and carbon budgets. Continued warming and stratification changes would have far-reaching effects on ocean heat content, sea-ice extent and thickness, ice-shelf stability, and at a broader scale an impact on global overturning circulation, oceanic CO_2 sequestration, sea-level rise and ultimately global climate regulation. These findings, combined with the interplay of anthropogenic forcing and sea ice variability, underscore the urgency of sustained, high-resolution monitoring across all sectors of the SO, providing critical benchmarks for improving and validating climate models.

Conflict of Interest

The authors declare no conflicts of interest relevant to this study.

Availability Statement

XBT data is available at Aulicino, Cotroneo, and Ferola et al. (2025). SLA information is provided by CMEMS (2023). Dynamic height referenced to 1500db is obtained from the World Ocean Atlas 2018 (https://odv.awi.de/data/ocean/world-ocean-atlas-2018/) and was processed via Ocean Data View software (Schlitzer, 2022). SAMW SST data were provided by the European Centre for Medium-Range Weather Forecasts (ECMWF) through the ERA5 reanalysis data set (ECMWF, 2023). Finally, the Argo float data used in this study were accessed through the Euro-Argo ERIC (2024) data selection tool.

Acknowledgments

This research is conducted within the framework of the Marine Observatory in the Ross Sea (MORSea), part of the Italian National Research Program in Antarctica (PNRA), which allowed the collection of an interesting 30 year time-series of temperature measurements in the upper 760 m of the SO from its northern boundary to Antarctica. Additional funding was provided by the PNRA19_0032 ACCESS project and the PNRA 18_00258 ESTRO project. The authors sincerely thank the scientists, technicians and ship crews involved in XBT sampling over the years, whose dedication made the collection of this valuable data set possible. Open access publishing facilitated by Universita degli Studi di Napoli Parthenope, as part of the Wiley - CRUI-CARE agreement.

References

Abram, N. J., Purich, A., England, M. H., McCormack, F. S., Strugnell, J. M., Bergstrom, D. M., et al. (2025). Emerging evidence of abrupt changes in the Antarctic environment. *Nature*, *644*(8077), 621–633. https://doi.org/10.1038/s41586-025-09349-5

Armour, K., Marshall, J., Scott, J., Donohoe, A., & Newsom, E. R. (2016). Southern Ocean warming delayed by circumpolar upwelling and equatorward transport. *Nature Geoscience*, *9*(7), 549–554. https://doi.org/10.1038/ngeo2731

Auger, M., Morrow, R., Kestenare, E., Sallée, J. B., & Cowley, R. (2021). Southern Ocean in-situ temperature trends over 25 years emerge from interannual variability. *Nature Communications*, *12*(1), 514. https://doi.org/10.1038/s41467-020-20781-1

Aulicino, G., Cotroneo, Y., & Ferola, A. I. (2025). XBT water column temperature data collected in the Southern Ocean between New Zealand and the Ross Sea during the austral summers from 1994/1995 to 2023/2024 [Dataset]. *Earth System Science Data*. *Zenodo*. https://doi.org/10.5281/zenodo.14848849

Aulicino, G., Ferola, A. I., Fortunato, L., Budillon, G., Castagno, P., Falco, P., et al. (2025). Expendable bathythermograph (XBT) data collected along the Southern Ocean chokepoint between Aotearoa/New Zealand and Antarctica, 1994–2024. *Earth System Science Data*, *17*(6), 2625–2640. https://doi.org/10.5194/essd-17-2625-2025

Bilbao, R. A., Gregory, J. M., Bouttes, N., Palmer, M. D., & Stott, P. (2019). Attribution of ocean temperature change to anthropogenic and natural forcings using the temporal, vertical and geographical structure. *Climate Dynamics*, *53*(9–10), 5389–5413. https://doi.org/10.1007/s00382-019-04910-1

Budillon, G., & Rintoul, S. R. (2003). Fronts and upper ocean thermal variability south of New Zealand. *Antarctic Science*, *15*(1), 141–152. https://doi.org/10.1017/S0954102003001135

Cai, W., Cowan, T., Godfrey, S., & Wijffels, S. (2010). Simulations of processes associated with the fast warming rate of the southern midlatitude ocean. *Journal of Climate*, *23*(1), 197–206. https://doi.org/10.1175/2009JCLI3081.1

Cai, W., Gao, L., Luo, Y., Li, X., Zheng, X., Zhang, X., et al. (2023). Southern Ocean warming and its climatic impacts. *Science Bulletin*, *68*(9), 946–960. https://doi.org/10.1016/j.scib.2023.03.049

Carter, L., Bostock-Lyman, H., & Bowen, M. (2022). Water masses, circulation and change in the modern Southern Ocean. In *Antarctic climate evolution* (2nd ed., pp. 165–197). Elsevier. https://doi.org/10.1016/B978-0-12-819109-5.00003-7

Cerrone, D., Fusco, G., Cotroneo, Y., Simmonds, I., & Budillon, G. (2017). The Antarctic Circumpolar wave: Its presence and interdecadal changes during the last 142 years. *Journal of Climate*, *30*(16), 6371–6389. https://doi.org/10.1175/JCLI-D-16-0646.1

Cerrone, D., Fusco, G., Simmonds, I., Aulicino, G., & Budillon, G. (2017). Dominant covarying climate signals in the Southern Ocean and Antarctic sea-ice influence during the last three decades. *Journal of Climate*, *30*(8), 3055–3072. https://doi.org/10.1175/JCLI-D-16-0439.1

Cheng, L., von Schuckmann, K., Abraham, J. P., Trenberth, K. E., Mann, M. E., Zanna, L., et al. (2022). Past and future ocean warming. *Nature Reviews Earth & Environment*, *3*(11), 776–794. https://doi.org/10.1038/s43017-022-00345-1

CMEMS - Copernicus Marine Environment Monitoring Service. (2023). Sea level anomaly (SLA) data from Ssalto/Duacs system [Dataset]. *Copernicus Marine Service*. https://doi.org/10.48670/moi-00148

Cotroneo, Y., Budillon, G., Fusco, G., & Spezie, G. (2013). Cold core eddies and fronts of the Antarctic Circumpolar Current south of New Zealand from in situ and satellite data. *Journal of Geophysical Research: Oceans*, *118*(5), 2653–2666. https://doi.org/10.1002/jgrc.20193

Cowley, R., & Krummel, L. (2022). *Australian XBT quality control cookbook version 2.1* (p. 89). CSIRO. (EP2022-1825). https://doi.org/10.25919/3tm5-zn80

de Brauwere, A., Jacquet, S. H., De Ridder, F., Dehairs, F., Pintelon, R., Schoukens, J., & Baeyens, W. (2007). Water mass distributions in the Southern Ocean derived from a parametric analysis of mixing water masses. *Journal of Geophysical Research*, *112*, C02021. https://doi.org/10.1029/2006JC003742

Euro-Argo ERIC. (2024). Argo float data selection tool [Dataset]. *Euro-Argo ERIC*. Retrieved from https://dataselection.euro-argo.eu

ECMWF - European Centre for Medium-Range Weather Forecasts. (2023). ERA5 reanalysis (single levels) [Dataset]. *Climate Data Store*. Retrieved from https://cds.climate.copernicus.eu/datasets/reanalysis-era5-single-levels

Falco, P., & Zambianchi, E. (2011). Near-surface structure of the Antarctic Circumpolar Current derived from World Ocean Circulation Experiment drifter data. *Journal of Geophysical Research*, *116*(C5), C05003. https://doi.org/10.1029/2010JC006349

Ferola, A. I., Cotroneo, Y., Wadhams, P., Fusco, G., Falco, P., Budillon, G., & Aulicino, G. (2023). The role of the Pacific-Antarctic Ridge in establishing the northward extent of Antarctic sea-ice. *Geophysical Research Letters*, *50*(10), e2023GL104373. https://doi.org/10.1029/2023GL104373

Fogt, R. L., & Marshall, G. J. (2020). The Southern Annular Mode: Variability, trends, and climate impacts across the Southern Hemisphere. *Wiley Interdisciplinary Reviews: Climate Change*, *11*(4), e652. https://doi.org/10.1002/wcc.652

Freeman, N. M., Lovenduski, N. S., & Gent, P. R. (2016). Temporal variability in the Antarctic Polar Front (2002–2014). *Journal of Geophysical Research: Oceans*, *121*(10), 7263–7276. https://doi.org/10.1002/2016JC012145

Fu, L.-L., Chelton, D. B., Le Traon, P.-Y., & Morrow, R. (2010). Eddy dynamics from satellite altimetry. *Oceanography*, *23*(4), 14–25. https://doi.org/10.5670/oceanog.2010.02

Gille, S. T. (1994). Mean sea surface height of the Antarctic Circumpolar Current from GEOSAT data: Methods and application. *Journal of Geophysical Research*, *99*(C9), 18255–18273. https://doi.org/10.1029/94JC01172

Gille, S. T. (2002). Warming of the Southern Ocean since the 1950s. *Science*, *295*(5558), 1275–1277. https://doi.org/10.1126/science.1065863

Gille, S. T. (2008). Decadal-scale temperature trends in the Southern Hemisphere ocean. *Journal of Climate*, *21*(18), 4749–4765. https://doi.org/10.1175/2008JCLI2131.1

Gille, S. T. (2014). Meridional displacement of the Antarctic Circumpolar Current. *Philosophical Transactions of the Royal Society A: Mathematical, Physical and Engineering Sciences*, *372*(2019), 20130273. https://doi.org/10.1098/rsta.2013.0273

Goes, M., Dong, S., Cowley, R., Cotroneo, Y., Sprintall, J., Cirano, M., et al. (2026). A high-resolution boundary current product from Gridded Observations of eXpendable BathyThermograph (XBT) transects. *Scientific Data*, *13*(1), 660. https://doi.org/10.1038/s41597-026-06883-3

Hersbach, H., Bell, B., Berrisford, P., Biavati, G., Horányi, A., Muñoz Sabater, J., et al. (2023). ERA5 hourly data on single levels from 1940 to present (Version 1). *Copernicus Climate Change Service (C3S) Climate Data Store*. Retrieved from https://cds.climate.copernicus.eu/datasets/reanalysis-era5-single-levels

Hu, X., Dong, S., & Goes, M. (2025). In situ temperature trends of the Antarctic Circumpolar Current south of South Africa. *Journal of Geophysical Research: Oceans*, *130*(12), e2025JC023030. https://doi.org/10.1029/2025JC023030

Li, Z., England, M. H., & Groeskamp, S. (2023). Recent acceleration in global ocean heat accumulation by mode and intermediate waters. *Nature Communications*, *14*(1), 6888. https://doi.org/10.1038/s41467-023-42468-z

Li, Z., England, M. H., Groeskamp, S., Cerovečki, I., & Luo, Y. (2021). The origin and fate of Subantarctic Mode Water in the Southern Ocean. *Journal of Physical Oceanography*, *51*(9), 2951–2972. https://doi.org/10.1175/JPO-D-20-0174.1

Li, Z., Groeskamp, S., Cerovečki, I., & England, M. H. (2022). The origin and fate of Antarctic Intermediate Water in the Southern Ocean. *Journal of Physical Oceanography*, *52*(11), 2873–2890. https://doi.org/10.1175/JPO-D-21-0221.1

Liu, W., Hegglin, M. I., Checa-Garcia, R., Li, S., Gillett, N. P., Lyu, K., et al. (2022). Stratospheric ozone depletion and tropospheric ozone increases drive Southern Ocean interior warming. *Nature Climate Change*, *12*(4), 365–372. https://doi.org/10.1038/s41558-022-01320-w

Liu, X., Meyer, A., & Chapman, C. C. (2024). Characteristics and trends of the Campbell Plateau meander in the Southern Ocean: 1993–2020. *Journal of Geophysical Research: Oceans*, *129*(2), e2023JC019876. https://doi.org/10.1029/2023JC019876

Lu, J., & Speer, K. (2010). Topography, jets, and eddy mixing in the Southern Ocean. *Journal of Marine Research*, *68*(3–4), 479–502. https://doi.org/10.1357/002224010794657227

Meijers, A. J. S., Le Quéré, C., Monteiro, P. M. S., & Sallée, J. (2023). Heat and carbon uptake in the Southern Ocean: The state of the art and future priorities. *Philosophical Transactions of the Royal Society A*, *381*(2249), 20220071. https://doi.org/10.1098/rsta.2022.0071

Menna, M., Cotroneo, Y., Falco, P., Zambianchi, E., Di Lemma, R., Poulain, P.-M., et al. (2020). Response of the Pacific Sector of the Southern Ocean to wind stress variability from 1995 to 2017. *Journal of Geophysical Research: Oceans*, *125*(10), e2019JC015696. https://doi.org/10.1029/2019JC015696

Naughten, K. A., Holland, P. R., & De Rydt, J. (2023). Unavoidable future increase in West Antarctic ice-shelf melting over the twenty-first century. *Nature Climate Change*, *13*(11), 1222–1230. https://doi.org/10.1038/s41558-023-01818-x

Olbers, D., Borowski, D., Völker, C., & Wölff, J.-O. (2004). The dynamical balance, transport and circulation of the Antarctic Circumpolar Current. *Antarctic Science*, *16*(4), 439–470. https://doi.org/10.1017/S0954102004002251

Orsi, A. H., Whitworth, T., & Nowlin, W. D. (1995). On the meridional extent and fronts of the Antarctic Circumpolar Current. *Deep-Sea Research Part I: Oceanographic Research Papers*, *42*(5), 641–673. https://doi.org/10.1016/0967-0637(95)00021-W

Purich, A., & England, M. H. (2021). Southern Annular Mode dynamics, trends, and impacts on the Southern Hemisphere climate system. *Nature Reviews Earth & Environment*, *2*, 505–520. https://doi.org/10.1038/s43017-021-00186-x

Rintoul, S. R. (2018). The global influence of localized dynamics in the Southern Ocean. *Nature*, *558*(7709), 209–218. https://doi.org/10.1038/s41586-018-0182-3

Roemmich, D., Church, J., Gilson, J., Monselesan, D., Sutton, P., & Wijffels, S. (2015). Unabated planetary warming and its ocean structure since 2006. *Nature Climate Change*, *5*(3), 240–245. https://doi.org/10.1038/nclimate2513

Sallée, J. B. (2018). Southern Ocean warming. *Oceanography*, *31*(2), 52–62. https://doi.org/10.5670/oceanog.2018.215

Sallée, J.-B., Pellichero, V., Akhoudas, C., Pauthenet, E., Vignes, L., Schmidtko, S., et al. (2021). Summertime increases in upper-ocean stratification and mixed-layer depth across the global ocean. *Nature*, *591*(7851), 592–598. https://doi.org/10.1038/s41586-021-03303-x

Sallée, J. B., Speer, K., & Rintoul, S. (2011). Mean-flow and topography control on surface eddy mixing in the Southern Ocean. *Journal of Marine Research*, *69*(4), 753–777. https://doi.org/10.1357/002224011799849408

Schlitzer, R. (2022). Ocean data view. http://odv.awi.de

Schmidtko, S., & Johnson, G. C. (2012). Multidecadal warming and shoaling of Antarctic Intermediate Water. *Journal of Climate*, *25*(1), 207–221. https://doi.org/10.1175/JCLI-D-11-00021.1

Shi, J., Xie, S., & Talley, L. D. (2018). Evolving relative importance of the Southern Ocean and North Atlantic in anthropogenic ocean heat uptake. *Journal of Climate*, *31*(18), 7459–7479. https://doi.org/10.1175/JCLI-D-18-0170.1

Silvano, A., Narayanan, A., Catany, R., Olmedo, E., González-Gambau, V., Turiel, A., et al. (2025). Rising surface salinity and declining sea ice: A new Southern Ocean state revealed by satellites. *Proceedings of the National Academy of Sciences of the United States of America*, *122*(27), e2500440122. https://doi.org/10.1073/pnas.2500440122

Sokolov, S., & Rintoul, S. R. (2007). Multiple jets of the Antarctic Circumpolar Current south of Australia. *Journal of Geophysical Research*, *112*(5), 1394–1412. https://doi.org/10.1175/JPO3111.1

Sokolov, S., & Rintoul, S. R. (2009a). Circumpolar structure and distribution of the Antarctic Circumpolar Current fronts: 1. Mean circumpolar paths. *Journal of Geophysical Research*, *114*(C11), C11018. https://doi.org/10.1029/2008JC005108

Sokolov, S., & Rintoul, S. R. (2009b). Circulation structure and distribution of the Antarctic Circumpolar Current fronts: 2. Variability and relationship to sea surface height. *Journal of Geophysical Research*, *114*, C11019. https://doi.org/10.1029/2008JC005248

Swart, N. C., Gille, S. T., Fyfe, J. C., & Gillett, N. P. (2018). Recent Southern Ocean warming and freshening driven by greenhouse gas emissions and ozone depletion. *Nature Geoscience*, *11*(11), 836–841. https://doi.org/10.1038/s41561-018-0226-1

Tan, Z., Cheng, L., Gouretski, V., Zhang, B., Wang, Y., Li, F., et al. (2023). A new automatic quality control system for ocean profile observations and impact on ocean warming estimate. *Deep-Sea Research Part I: Oceanographic Research Papers*, *194*, 103961. https://doi.org/10.1016/j.dsr.2022.103961

Thompson, A. F., & Naveira Garabato, A. C. (2014). Equilibration of the Antarctic Circumpolar Current by standing meanders. *Journal of Physical Oceanography*, *44*(7), 1811–1828. https://doi.org/10.1175/JPO-D-13-0163.1

Thompson, A. F., & Sallée, J. B. (2012). Jets and topography: Jet transitions and the impact on transport in the Antarctic Circumpolar Current. *Journal of Physical Oceanography*, *42*(6), 956–972. https://doi.org/10.1175/JPO-D-11-0135.1

Wang, G., Cai, W., & Gao, L. (2017). Recent wind-driven change in Subantarctic Mode Water and its impact on Southern Hemisphere ocean heat storage. *Nature Climate Change*, *7*, 902–907. https://doi.org/10.1038/s41558-017-0022-8

Wang, Z., Li, Y., Shi, J., Zhang, Z., Liu, C., Zhou, M., & Wei, Z. (2025). Water masses in the Southern Ocean: Variability, trends, and drivers. *Acta Oceanologica Sinica*, *44*(3), 35–56. https://doi.org/10.1007/s13131-024-2442-4

Wyatt, J., Bindoff, N. L., Foppert, A., Phillips, H. E., & Rintoul, S. R. (2025). Observed trends and variability in the water masses of the Southern Ocean. *ESS Open Archive*. https://doi.org/10.22541/essoar.176521551.16490272/v1

Zambri, B., Solomon, S., Thompson, D. W. J., & Fu, Q. (2021). Emergence of Southern Hemisphere stratospheric circulation changes in response to ozone recovery. *Nature Geoscience*, *14*(9), 638–644. https://doi.org/10.1038/s41561-021-00803-3